Biochimica et Biophysica Acta, 645 (1981) 318–326
Elsevier/North-Holland Biomedical Press

BBA 79312

EFFECTS OF *n*-ALKANES ON THE MORPHOLOGY OF LIPID BILAYERS

A FREEZE-FRACTURE AND NEGATIVE STAIN ANALYSIS

T.J. McINTOSH and M.J. COSTELLO

Department of Anatomy, Duke University Medical Center, Durham, NC 27710 (U.S.A.)

(Received January 29th, 1981)

Key words: n-Alkane; Freeze-fracture; Negative stain; Lipid bilayer; Morphology

The effect of *n*-alkanes on the ultrastructure of lipid bilayers has been investigated using freeze-fracture and negative stain electron microscopy. It has been found that the morphology of bilayers containing the long alkane tetradecane is quite different from bilayers containing the short alkane hexane. The smooth fracture faces of gel and liquid crystalline state bilayers are unmodified by tetradecane. However, hexane dramatically alters the hydrophobic bilayer interior, producing large (20 to 50 nm) mounds and depressions in the fracture faces. The fracture steps in these multilayer preparations containing hexane are variable in thickness and often considerably wider than the corresponding fracture steps in multilayers which contain tetradecane or are solvent-free. Alkanes also modify the structure of the $P_{\beta'}$ or 'banded' phase of phosphatidylcholine bilayers. The incorporation of tetradecane removes the banded structure from both the bilayer's hydrophilic surface, as viewed by negative staining, and the bilayer's hydrophobic interior, as viewed by the freeze-fracture technique. These results are consistent with X-ray diffraction data which imply that long alkanes are primarily located between adjacent lipid hydrocarbon chains in each monolayer of the bilayer, while short alkanes can partition into the geometric center of the bilayer between apposing monolayers.

Introduction

The manner in which the *n*-alkanes interact with lipid bilayers is of interest for several reasons. The *n*-alkanes, especially the shorter ones, are anesthetics and have other pharmacological effects [1,2], at least some of which have been attributed to their interaction with the bilayer [3]. The *n*-alkanes are also used extensively to form the planar black lipid membranes employed in electro-physiological studies [4]. Significantly, the properties of the black lipid films depend strongly on the length of the *n*-alkane used. Membranes formed with the small alkanes, such as hexane (six carbons), are markedly thicker than bilayers formed from larger alkanes, such as tetradecane (fourteen carbons) [5–7]. In addition, the membrane conductances of bilayers treated with certain ionophores depend on the length of the alkane solvent [8].

Recently, the effects of *n*-alkanes on the properties and structure of vesicular bilayers have been analyzed [9,10]. It has been found by ^{1}H-NMR spectroscopy [9] and by differential scanning calorimetry [10] that small and long alkanes have quite distinct effects on the phase transitions of phosphatidylcholine bilayers, with the short alkanes decreasing and the longer alkanes increasing the phase transition temperature. X-ray diffraction data [10] showed differences in repeat periods and in electron density profiles for multiwalled vesicles containing short and long alkanes. These X-ray and calorimetric data were interpreted to mean that the long alkanes tend to align parallel to the lipid hydrocarbon chains, while the short alkanes are located in the geometric center of the bilayer as well as intercalated between the lipid hydrocarbon chains [10].

This present investigation, using freeze-fracture and negative stain electron microscopy, was undertaken to provide further information on the localization of the *n*-alkanes in lipid bilayers and also to answer some specific questions concerning the properties and structure of bilayers containing *n*-alkanes. Freeze-fracture is unique among morphological techniques in that it provides a view of the hydrophobic interior of lipid bilayers [11]. Because the short alkanes, but not the long alkanes, are thought to localize in the geometric center of the bilayer, we were interested in observing the differences in appearance of fracture faces from bilayers containing alkanes of different length. In our experiments, we have used hexane and tetradecane as examples of short and long alkanes, respectively. Also, since long alkanes eliminate the chain tilt from gel state bilayers [12,13] and since it has been proposed [12–14] that chain tilt is necessary for the occurrence of the $P_{\beta'}$ or two-dimensional 'banded' phase of phosphatidylcholine bilayers [15–17], we wanted to determine if bilayers treated with tetradecane have the 'banded' structure.

Materials and Methods

The synthetic lipids used in these experiments, dipalmitoyl phosphatidylcholine (DPPC) and dimyristoyl phosphatidylcholine (DMPC), were used as obtained from Sigma or Calbiochem. Egg lecithin was obtained in chloroform/methanol from Lipid Products (Nuttfield, U.K.). The *n*-alkanes solvents (99% pure) were purchased from Sigma. Triple distilled water was used in all experiments.

The lipid/alkane/water suspensions were made by the following procedure. In the case of the egg lecithin, the chloroform/methanol was removed by a two-step procedure involving an initial removal with a rotary evaporator and then a 1-h period under high vacuum. The dry lipids were placed in a small V-bottomed reaction vial, and appropriate amounts of *n*-alkane were added. Since we were interested in studying the morphology of bilayers saturated with the various alkanes, we used concentrations which provided excess alkane in the suspension [10]. The mole fraction of alkane listed in each figure caption refers to the amount of alkane added to the reaction vial, and does not indicate the amount of alkane adsorbed by the lipid. The lipid/alkane suspension was vortexed until thoroughly mixed, and then water was added. Unless otherwise noted in the figure captions, we used 70% water relative to weight of the lipid. The lipid/alkane/water suspension was mixed by extensive vortexing and allowed to equilibrate for several hours at a temperature above the lipid phase transition temperature. The suspensions were then allowed to equilibrate for several hours at the temperature at which the experiment was to be performed.

Freeze-fracture was done by the technique described earlier [18,19]. Small samples (0.1 μl), prepared without cryoprotectants, were sandwiched between two copper strips to give a sample thickness of about 10 μm. The sandwiches were plunged into liquid propane (–190°C) at sample cooling rates in excess of 10 000°C/s (from 0 to –100°C; see Ref. 19). Frozen samples were inserted into a hinged double replica device adapted for use on a Balzers BA 360 freeze-fracture unit. Fracturing was done at –150°C and about 10^{-7} torr by releasing a spring which opened the sandwiches. Samples were immediately replicated with platinum from a 45° angle and carbon from a 90° angle. Replicas were cleaned in organic solvents such as chloroform/ethanol and picked up on uncoated 400 mesh electron microscope grids. Freeze-fracture micrographs are mounted so that the metal deposition direction is from the bottom.

Negative staining was performed by diluting the specimen with a drop of water, placing the diluted specimen on a carbon-coated electron microscope grid, adding a small drop of 2% uranyl acetate in water, and blotting dry. Before use, the uranyl acetate, the water used for diluting the sample, and the sample itself were kept at the temperature of experimental interest.

All specimens were examined with a Philips 301 electron microscope equipped with an anticontamination device cooled with liquid nitrogen.

Results

Fig. 1A presents a typical freeze-fracture image of DPPC in the gel state below the pretransition temperature. Several fracture steps are seen and the fracture faces are quite smooth. For DPPC with added tetradecane, the fracture faces are also smooth (Fig. 1B)

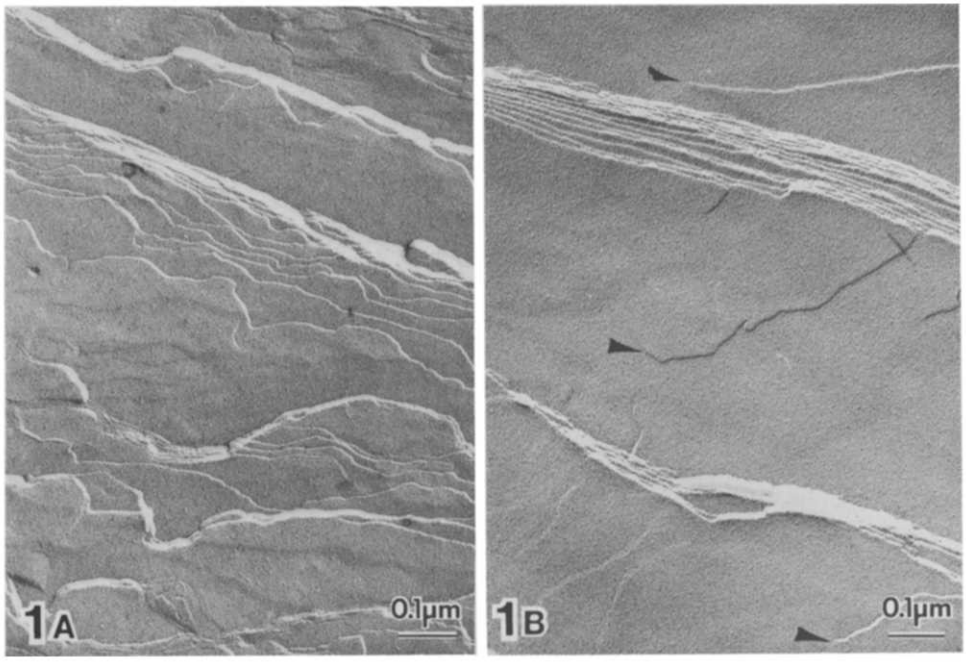

Fig. 1. Freeze-fracture images of: (A) DPPC in 30% water and (B) DPPC/tetradecane (0.75 mol fraction tetradecane) in 30% water. Both samples were quenched from 18°C, which is below the pretransition temperature of DPPC. Several fracture steps of uniform thickness are seen in both (A) and (B). Note that screw dislocations [25] are present in both samples, but seem to be more numerous in B (arrowheads).

and the fracture steps are of uniform height. However, fracture faces from DPPC with incorporated hexane have a quite different appearance. As shown in Fig. 2 A, B, and C, the fracture faces of DPPC/hexane membranes are covered with interconnecting ridges which surround mounds or depressions of variable size, but usually on the order of 20 to 50 nm in diameter. The fracture steps in these DPPC/hexane preparations tend to be more variable in thickness than the corresponding fracture steps in DPPC bilayers with the tetradecane (Fig. 1B) or solvent-free DPPC bilayers (Fig. 1A). That is, at the same shadowing angle, the fracture step can cast a large shadow (Fig. 2B, large arrowhead) or relatively small shadow (Fig. 2B, small arrowhead). In Fig. 2C, the fracture step shows a notable thickening and thinning. The width of the fracture step is related to whether the fracture passes directly through one of the mounds or at the perimeter of a mound.

For temperatures between the pretransition and main transition, synthetic phosphatidylcholines have been shown to have a banded structure in freeze-fracture images [17]. Figs. 3A and 3B show this banded structure with a spacing of about 13 nm for DMPC at 18°C. There are, as seen in previous studies [16,17], occasional regions where the periodicity is approximately twice as large and the depth of the banding is also greater (inset, Fig. 3A). When tetradecane is added to DMPC, the rippled structure is not present and smooth fracture faces are observed (Fig. 3C) at 18°C. Differential scanning calorimetry has shown that tetradecane abolishes the thermal pretransition [10].

The banded structure can also be observed by negative staining techniques. Figs. 4A and 4B show images of DMPC negatively stained at 18°C, while Fig. 4C shows a DMPC/tetradecane mixture at 18°C. The DMPC bilayers clearly display a banded structure, while the DMPC/tetradecane liposomes are smooth. In Fig. 4B, the linearity of the $P\beta'$ phase is apparent, while in Fig. 4A two layers of the negatively stained banded structure are superimposed,

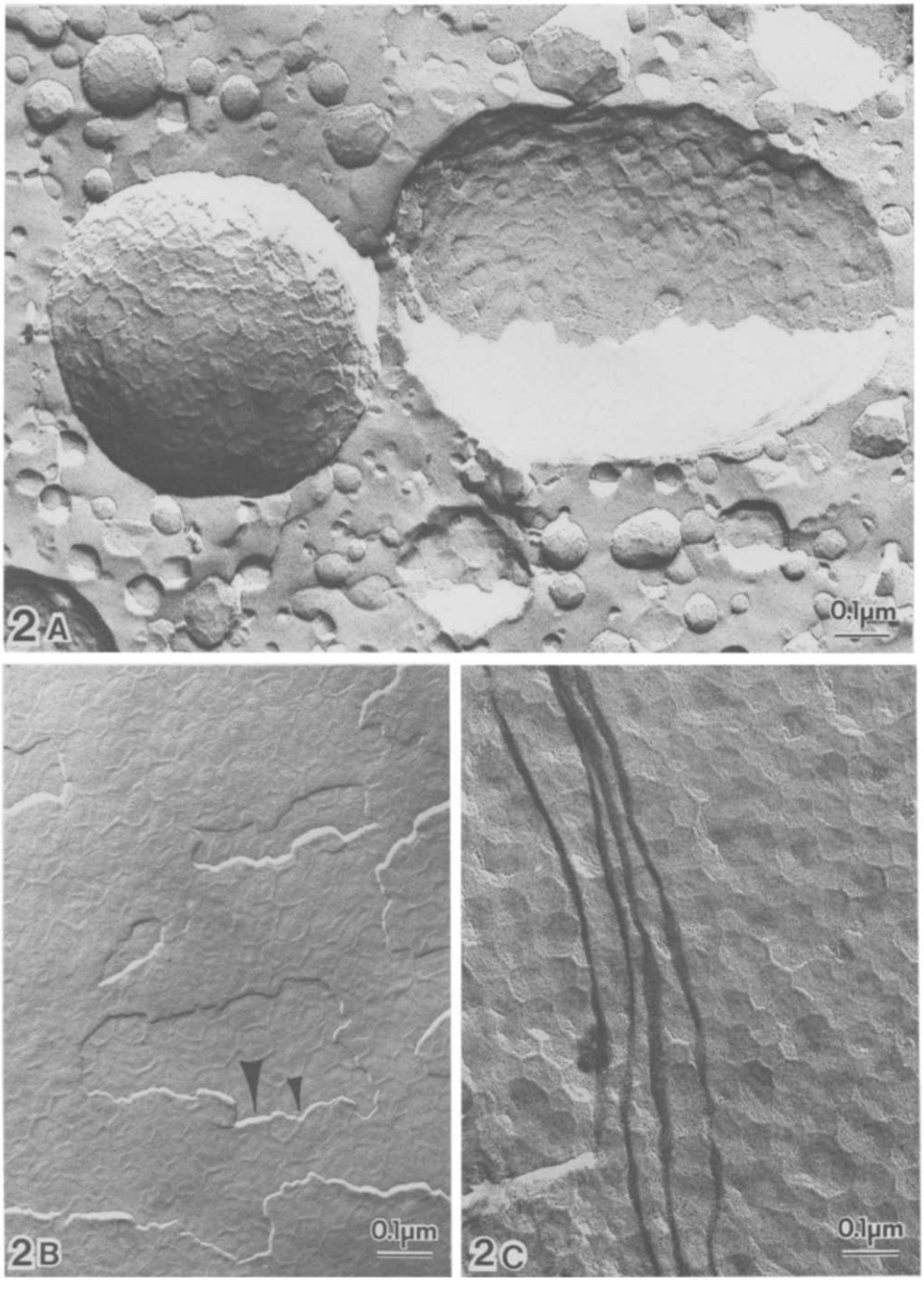

Fig. 2. Freeze-fracture images of DPPC containing hexane (0.75 mol fraction hexane). (A) Large convex vesicle displays a ridged pattern and large concave vesicle contains ring-shaped mounds and depressions. The patterns in the smaller vesicles are not as clear, probably due to the high curvature. All vesicles are embedded in a smooth ice background. (B) Ridged outlines are seen on extended fracture faces of a large multiwalled vesicle. Fracture steps show a variation in thickness depending on whether the steps occur at a mound (thick step, large arrowhead) or a ridge between mounds (thin step, small arrowhead). (C) Variation in thickness of fracture steps can be seen in this view of a large multilamellar vesicle in which the depressions are evident.

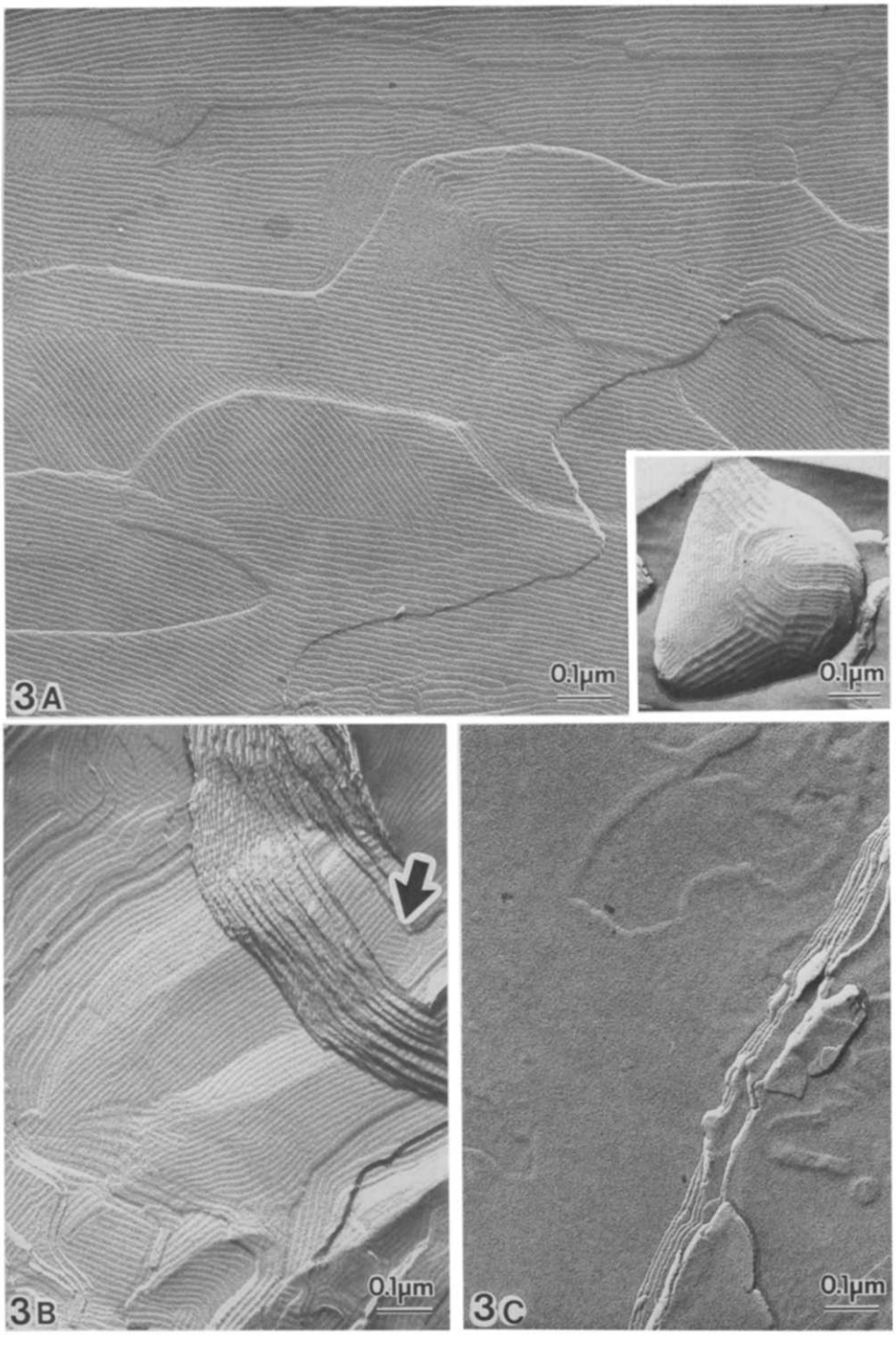

Fig. 3. (A) and (B). Freeze-fracture images of DMPC quenched from 18°C, which is between the pretransition and main transition temperatures. The banded pattern of the $P\beta'$ phase is evident with the spacing between bands being 13 nm. Occasionally a vesicle is seen which contains a spacing which is approximately twice as large (inset to A). In (B) the edge fractures in a multilamellar vesicle reveal the correspondence of the banded pattern between layers (arrow marks a mosaic region which is observable through several layers). (C) The addition of tetradecane (0.75 mol fraction in DMPC) eliminated the banded pattern.

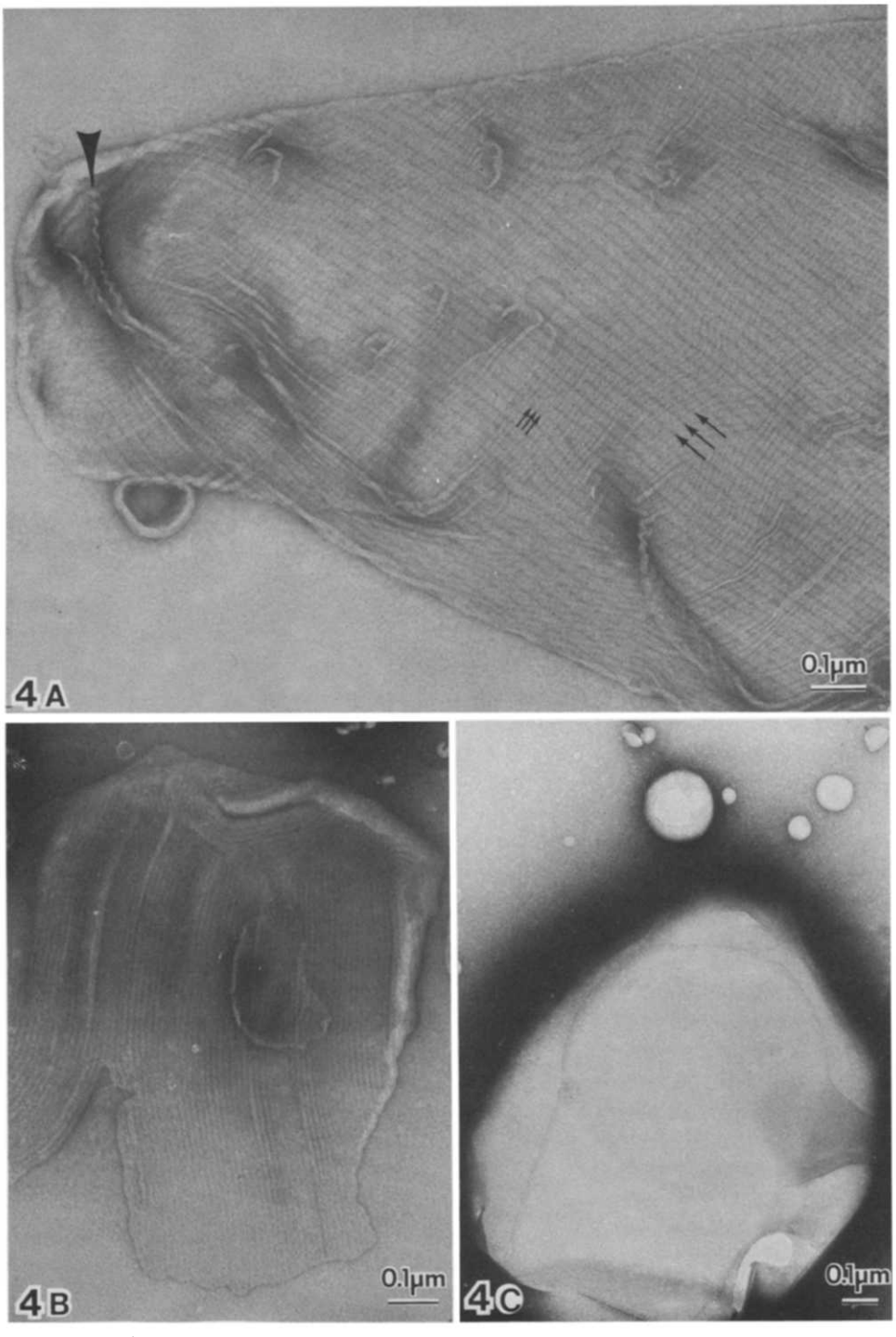

Fig. 4. (A) and (B). Negative stain images of DMPC vesicles at 18°C. (A) A large collapsed vesicle shows the superposition of banded patterns from two bilayers. The bands with the wider spacing (approx. 26 nm, large arrows) are nearly perpendicular to the narrow spaced bands (13 nm, small arrows). The banded pattern can be seen in edge view in regions where there are folds in the bilayer (arrowhead). (B) A fragment of a vesicle shows bands at a 13-nm specing. (C) The addition of tetradecane (0.75 mol fraction in DMPC) produces vesicles with smooth surfaces.

producing a two-dimensional network. In the middle of Fig. 4A one observes a bilayer with a banding of 13 nm periodicity going from lower left to upper right superimposed on another bilayer with a 26 nm periodicity going from upper left to lower right. Of particular interest in this image are the edges of the vesicle and folds in the vesicle (arrowhead) where the large periodicity banded structure can be seen in side view. In control experiments only smooth surfaces are observed in DMPC liposomes negatively stained at temperatures above the main transition temperature. For vesicles cooled below the pretransition temperature, an occasional area of rippled structure can be found, similar to freeze-fracture images of Luna and McConnell [17].

The effect of *n*-alkanes on bilayers in the liquid-crystalline state are shown in Fig. 5. Egg lecithin bilayers have flat fracture faces (Fig. 5A). These faces have a slight granular texture and are not as smooth as gel state DPPC (Fig. 1A). Tetradecane does not modify the flatness of these fractures faces (data not shown). However, the fracture faces from egg lecithin/hexane bilayers have a quite different appearance (Fig. 5B). Irregularly shaped rounded ridges cover most fracture planes. The fracture steps are irregular in height, being thickest where the step passes through the middle of one of the rounded ridges (Fig. 5B, arrow).

Discussion

Freeze-fracture experiments have shown that the long alkane tetradecane and the short alkane hexane have markedly different effects on the hydrophobic interior of lipid bilayers. Bilayers containing tetradecane have smooth fracture faces and fracture steps which are uniform in thickness (Fig. 1B), much like control bilayers (Fig. 1A). The similarities in freeze-fracture images of bilayers with and without tetradecane are consistent with the interpretation from X-ray diffraction data [10], that the long alkanes align parallel to the lipid hydrocarbon chains. Such a positioning of the alkanes would not be expected to modify the appearance of the fracture planes, which

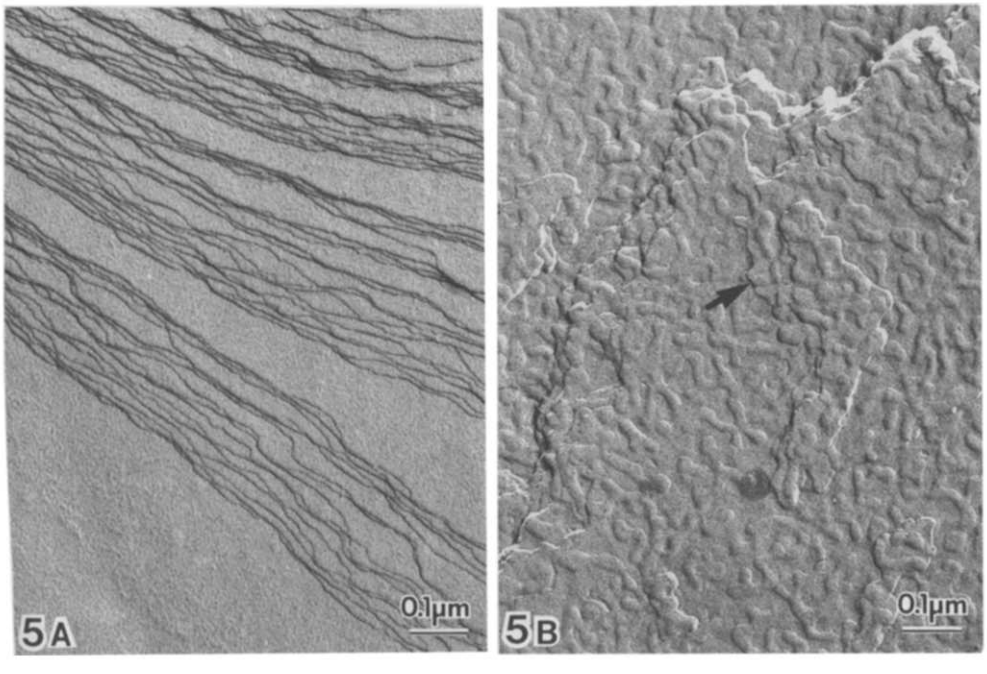

Fig. 5. (A) Freeze-fracture image of egg lecithin quenched from 18°C shows a multilamellar region with smooth surface and uniform step heights. (B) The addition of hexane (0.83 mol fraction hexane in egg lecithin) produces irregularly shaped ridges and fracture steps of variable thickness. Large steps (arrow) are often seen passing through ridges.

have been shown to pass through the geometric center of lipid bilayers [11,20]. The long alkanes do have the effect of eliminating chain tilt from gel state phosphatidylcholine bilayers [12,13]. Although the presence or absence of chain tilt cannot be demonstrated directly with the freeze-fracture technique, one structural effect of chain tilt loss can be observed. The banded structure of the $P\beta'$ phase of synthetic phosphatidylcholine bilayers occurs at temperatures between the pretransition and the main transition for lipids with tilted chains. The long alkanes remove the chain tilt [12,13], the pretransition [10], and as shown in Figs. 3 and 4, the banded structure from phosphatidylcholine bilayers. Thus, using the notation of Luzzati and co-workers [12], the long alkanes convert DMPC from either an $L\beta'$ phase (below the pretransition temperature) or $P\beta'$ phase (between the pretransition and main transition) to an $L\beta$ phase (with no pretransition).

Fracture faces from bilayers containing hexane are not smooth, but have mounds, depressions, and/or ridges, the exact morphology depending on whether the lipid is in the gel (Fig. 2) or liquid crystalline states (Fig. 5B). The modification of the fracture face is consistent with the interpretation [10] that short alkanes can reside in the geometric center of the bilayer. The large and variable width of the fracture steps is compatible with the results from X-ray diffraction experiments [10], where the diffraction lines obtained from DPPC/hexane and egg lecithin/hexane bilayers were broader and of larger repeat period than those from control, solvent-free bilayers. It seems certain that the mounds and depressions are caused in some manner by the hexane. The images, such as those in Fig. 2, are reproducible and are quite different from the controls. To the best of our knowledge, such images have never been reported under any other circumstances. The variability in the width of the fracture steps (Figs. 2B and 2C) and the large dimensions of the steps at their widest points, taken together with the fact that hexane has an extremely low solubility in water, are strong indications that significant amounts of hexane exist in the center of the bilayer. However, it may be that the exact shape of the interconnecting ridges of Figs. 2 A, B, and C is caused in part by the freeze-fracture process. For example, the ultra-rapid freezing rates that we are using are fast enough that vitreous ice forms between vesicles (see Refs. 18 and 19); however, it is still possible that there could be a rearrangement of hexane and/or a formation of hexane crystals in the center of the bilayer during the freezing process.

The reasons for the difference in appearance between the fracture faces from DPPC/hexane and egg lecithin/hexane are not known, although they presumably relate to differences in properties of gel and liquid-crystalline state lipids. One possibility is that the difference in hydrocarbon chain structure between the gel and liquid-crystalline states might influence the amount of hexane which can be absorbed into the geometric center of the bilayer. According to X-ray diffraction data [10], the repeat period of DPPC and egg lecithin increase by similar amounts with the incorporation of hexane. (The diffraction data also show that DPPC remains in the gel state and egg lecithin remains in the liquid-crystalline state with incorporated hexane.) However, in hydrated control bilayers, DPPC has rigid, extended hydrocarbon chains while the chains of egg lecithin are kinked and less rigid. Thus, it is possible in the case of egg lecithin/hexane bilayers that some of the hydrocarbon chains of egg lecithin can unfold and extend far into the hexane region in the center of the bilayer [21]. This could drastically alter the properties of this hexane region.

To the best of our knowledge, the images in Figs. 4A and 4B are the first time the $P\beta'$ phase has been observed with the negative stain technique. The negative stain apparently forms a cast over the lipid layers and the banded structure is preserved, even though the specimens are dehydrated and heated in the electron beam of the microscope. The banded structure has been employed in the past as an aid in observing lipid-lipid and lipid-protein interactions [22,23] by the freeze-fracture technique. Some of these types of interactions can also be studied by negative staining, which offers some advantages. First, the negative staining techniques is simple, fast, and does not require elaborate preparatory apparatus. Secondly, new information can be obtained, as the hydrophilic surface of the bilayer is observed and, in folds in the bilayer (Fig. 4A, arrow), the banded structure can be seen in side-view. The images of Figs. 4A and 4B are consistent with 'rippled' structural models of Tardieu et al. [12] and Janiak et al. [24], but inconsistent with a 'saw-tooth' or 'peristaltic' model [24].

Acknowledgements

We thank Dr. Guido Zampighi for suggesting the negative stain experiments. We are grateful to Ms. Susan Hester and Ms. Mary Sheedy for technical assistance. This work was supported by NIH grants RO1 GM27278 (to T.J.M.) and RO1 GM27914 (to M.J.C.).

References

1 Carter, D.E. and Fernando, W. (1979) J. Chem. Educ. 56, 284–288
2 Haydon, D.A., Hendry, B.M., Levinson, S.R. and Requena, J. (1977) Biochim. Biophys. Acta 470, 17–34
3 Haydon, D.A., Hendry, B.M., Levinson, S.R. and Requena, J. (1977) Nature 268, 356–358
4 Tien, H.T. (1974) Bilayer Lipid Membranes, Theory and Practice, Marcel Dekker, New York
5 White, S.H. (1977) Ann. N.Y. Acad. Sci. 303, 243–265
6 Benz, R., Frölich, O., Läuger, P. and Montal, M. (1975) Biochim. Biophys. Acta 394, 323–334
7 Fettiplace, R., Andrews, D.M. and Haydon, D.A. (1971) J. Membrane Biol. 5, 277–296
8 Hendry, B.M., Urban, B.W. and Haydon, D.A. (1978) Biochim. Biophys. Acta 513, 106–116
9 Hunt, G.R. and Tipping, L.R.H. (1978) Biochim. Biophys. Acta 507, 242–261
10 McIntosh, T.J., Simon, S.A. and MacDonald, R.C. (1980) Biochim. Biophys. Acta 597, 445–463
11 Branton, D. (1966) Proc. Natl. Acad. Sci. USA 55, 1048–1056
12 Tardieu, A., Luzzati, V. and Reman, F.C. (1973) J. Mol. Biol. 75, 711–735
13 McIntosh, T.J. (1980) Biophys. J. 29, 237–246
14 Gebhardt, C., Gruler, M. and Sackmann, E. (1977) Z. Naturforsch. 32c, 581–596
15 Janiak, M.J., Small, D.M. and Shipley, G.G. (1976) Biochemistry 15, 4575–4580
16 Ververgaert, P.H.J., Elberg, P.F., Luitingh, A.J. and Van den Berg, H.J. (1972) Cytobiologie 6, 86–96
17 Luna, E.J. and McConnell, H.M. (1977) Biochim. Biophys. Acta 466, 381–392
18 Costello, M.J. and Corless, J.M. (1978) J. Microscopy 112, 17–37
19 Costello, M.J. (1980) Scanning Electron Microscopy II, 361–370
20 Deamer, D.W. and Branton, D. (1967) Science 158, 655–657
21 White, S.H. (1979) Biophys. J. 25, 9a
22 Stewart, T.P., Hui, S.W., Portis, A.R. and Papahadjopoulos, D. (1979) Biochim. Biophys. Acta 556, 1–16
23 Kleeman, W. and McConnell, H.M. (1976) Biochim. Biophys. Acta 419, 206–222
24 Janiak, M.J., Small, D.M. and Shipley, G.G. (1979) J. Biol. Chem. 254, 6068–6078
25 Kleman, M., Williams, C.E., Costello, M.J. and Gulik-Krzywicki, T. (1977) Philos. Mag. 35, 33–56